Processing of progranulin into granulins involves multiple lysosomal proteases and is affected in frontotemporal lobar degeneration

Swetha Mohan

   University of California San Francisco

Paul J. Sampognaro

   University of California San Francisco

Andrea R. Argouarch

   University of California San Francisco

Jason C. Maynard

   University of California San Francisco

Anand Patwardhan

   University of California San Francisco

Mackenzie Welch

   University of California San Francisco

Emma C. Courtney

   University of California San Francisco

Jiasheng Zhang

   University of California San Francisco

Amanda Mason

   University of California San Francisco

Kathy H. Li

   University of California San Francisco

Eric J. Huang

   University of California San Francisco

William W. Seeley

   University of California San Francisco

Bruce L. Miller

   University of California San Francisco

Alma Burlingame

   University of California San Francisco

Mathew P. Jacobson

   University of California San Francisco

Aimee Kao (✉ Aimee.Kao@UCSF.EDU)

University of California San Francisco   https://orcid.org/0000-0002-7686-7968

Research article

Keywords: Progranulin, granulin, frontotemporal lobar degeneration, lysosome, protease, pH, asparagine endopeptidase

---

Abstract

Background - Progranulin loss-of-function mutations are linked to frontotemporal lobar degeneration with TDP-43 positive inclusions (FTLD-TDP-*Pgrn*). Progranulin (PGRN) is an intracellular and secreted pro-protein that is proteolytically cleaved into individual granulin peptides, which are increasingly thought to contribute to FTLD-TDP-*Pgrn* disease pathophysiology. Intracellular PGRN is processed into granulins in the endo-lysosomal compartments. Therefore, to better understand the conversion of intracellular PGRN into granulins, we systematically tested the ability of different classes of endo-lysosomal proteases to process PGRN at a range of pH setpoints.

Results - *In vitro* cleavage assays identified multiple enzymes that can process human PGRN into multi- and single-granulin fragments in a pH-dependent manner. We confirmed the role of cathepsin B and cathepsin L in PGRN processing and showed that these and several previously unidentified lysosomal proteases (cathepsins E, G, K, S and V) are able to process PGRN in distinctive, pH-dependent manners. In addition, we have demonstrated a new role for asparagine endopeptidase (AEP) in processing PGRN, with AEP having the unique ability to liberate granulin F from the pro-protein. Brain tissue from individuals with FTLD-TDP-*Pgrn* show increased PGRN processing to granulin F and an increased activity of AEP, in a region-specific manner.

Conclusions - This study demonstrates that multiple lysosomal proteases may work in concert to liberate multi-granulin fragments and granulins. It also implicates both AEP and granulin F in the neurobiology of FTLD-TDP-*Pgrn*. Modulating progranulin cleavage and granulin production may represent therapeutic strategies for FTLD-*Pgrn* and other progranulin-related diseases.

Background

Progranulin (PGRN) is an evolutionarily conserved glycoprotein with functions in inflammation, wound healing, tumorigenesis, and neuroprotection [1,2]. Dosage of PGRN plays a central role in its cellular functions as haploinsufficiency of PGRN leads to an adult-onset neurodegenerative disorder, frontotemporal lobar degeneration (FTLD-TDP-*Pgrn*), while complete loss of PGRN leads to a childhood lysosomal storage disorder called neuronal ceroid lipofuscinosis (NCL) [3–5]. As a molecule with complex layers of regulation, PGRN can also be proteolytically cleaved into multiple biologically active, disulfide-rich peptides known as granulins which, in some instances, have contrasting functions to its precursor [6–10]. Although granulins were identified before PGRN, the regulation of granulin production remains poorly understood [11]. Since haploinsufficiency of PGRN protein could potentially also affect granulin levels, understanding granulin production may shed light on how partial loss of PGRN causes age-associated neurodegeneration.

Proteolytic processing of PGRN liberates up to eight granulin peptides, named paragranulin (~3.5kD) and granulins A through G (~7kD each) (Fig. 1a). Fragments consisting of multiple granulins have also been previously described [12,13], and these multi-granulin fragments (MGFs) exert biological activities

as well [14]. PGRN is secreted into the extracellular matrix where proteases, such as neutrophil elastase, may process PGRN [6,8,15]. Intracellularly, PGRN localizes to endo-lysosomes and recent studies have shown that intracellular processing of PGRN into granulins also occurs in the endo-lysosomal compartments [16–20]. The lysosomal cysteine proteases, cathepsins B (CTSB) and L (CTSL), were identified as PGRN proteases in human and mouse models [17,19,20]. However, a comprehensive study of intracellular PGRN proteases has not yet been performed.

To better understand the intracellular processing of PGRN into granulins, we set out to catalog the endo-lysosomal proteases that regulate PGRN processing into granulins. Using *in vitro* protease cleavage assays, we identified multiple lysosomal proteases that can process PGRN to multi-granulin fragments and individual granulins. Interestingly, they did so in a pH-dependent manner that is distinctive depending on the protease. In a neuronal cell model, we validated the known roles for CTSB and CTSL and showed that asparagine endopeptidase (AEP, also known as legumain) is a novel PGRN protease that can specifically liberate granulin F. Finally, comparing human brain lysates from control and FTLD-TDP-*Pgrn* subjects, we show a significant increase in the production of granulin F and an increased activity of AEP in degenerating regions of the brain. This study is the first to systematically identify a suite of endo-lysosomal proteases that likely work in concert to process PGRN to granulins and reveals AEP as a new PGRN protease with relevance in FTLD-TDP. It also reveals the bioactive MGFs and granulins that can be produced by each protease, which could become important in the development of FTLD-*Pgrn* therapies targeted at preventing PGRN cleavage.

Methods

In vitro cleavage assay

For *in vitro* cleavage assays, 400ng of recombinant human progranulin (R&D #CF-2420) was incubated with or without 1μM of each protease. Depending on the pH setpoint, the following buffers were used: 100mM sodium citrate pH 3.4, 50mM sodium acetate pH 4.5 or 5.5, 50mM 2-(N-morpholino)-ethanesulfonic acid (MES) buffer pH 6.5, 100mM phosphate buffer saline (PBS) pH 7.4 with 1mM EDTA and 2mM DTT for 20 or 60 minutes at 37°C water bath. The cleavage was performed in a total volume to 19.5μl. Protease activity was stopped by adding 7.5μl of NuPAGE 4X LDS (Fisher #NP0007), 3μl of 10X reducing agent (i.e. 50μM) (Fisher #NP0009) and denatured for 10 minutes at 70°C. Of note, we used these denaturing conditions to reduce the potential for dimerization of fragments (a known possibility with PGRN) [21].

For the time-course assays, 400ng of recombinant human progranulin (R&D #CF-2420) was incubated with 50nM or 1uM of the enzyme indicated in the same reaction conditions as mentioned above. The reaction was allowed to proceed for the time-point indicated. The reaction was stopped at mentioned above.

All samples were run on precast NOVEX 4-12% Bis-Tris gels (Fisher #NP0321PK2) using MES buffer (Fisher #NP0002). The gel was then either fixed in 40% ethanol and 10% acetic acid for silver and

coomaisse staining or transferred onto nitrocellulose membranes for western blotting analysis.

Silver stain - Silver staining was performed according to manufacturer's instructions with SilverQuest silver staining kit (Thermo #LC6070).

Coomassie stain - Coomassie staining was done using BIO-RAD QC colloidal coomaisse stain (Bio-rad #160-0803). The gel was stained overnight and was removed by washing in milli-Q water for 3 hours.

Recombinant proteases - Cathepsin E (R&D #1294-AS), Cathepsin D (R&D #1014-AS), Napsin A (R&D #8489-NA), Cathepsin G (Millipore #219873), Cathepsin A (R&D #1049-SE), Pro-X-carboxypeptidase (R&D #7164-SE-010), Cathepsin L (Millipore #219402), Cathepsin B (Millipore #219364), Cathepsin K (Millipore #219461), Cathepsin S (R&D #1183-CY), Cathepsin V (R&D #1080-CY), Asparagine endopeptidase/legumain (R&D #2199-CY), Cathepsin H (R&D #7516-CY-010), Cathepsin C (R&D #1071-CY), Cathepsin O (Abcam #ab267932), Cathepsin F (Abcam #ab240858), and Cathepsin X (R&D #934-CY).

Protease activation and confirmation of activity – Cathepsins E, D, G, L, B, K, S, V, F, and O as well as Asparagine endopeptidase, Napsin A, and Pro-X-carboxypeptidase require no activation, according to the vendor, and were used as purchased. Cathepsin A, C, and H require pre-activation before use. For cathepsin A and cathepsin C activation, 1µM of each protease was incubated with 200nM of cathepsin L at room temperature for 1 hour. After 1 hour, 50µM of benzyloxycarbonyl FY(*t*-Bu)-DMK, an irreversible, highly specific inhibitor of cathepsin L (Sigma # 219427) was added to quench cathepsin L activity. Once activated, cathepsin A and C were used in the experiments outlined. Similarly, for cathepsin H activation, 1µM of cathepsin H was incubated with 500nM of Thermolysin (R&D # 3097-ZN) at room temperature for 3 hours. After 3 hours, 1mM of Phosphoramidon (Tocris # 6333), a specific thermolysin inhibitor, was added to quench Thermolysin activity. Once activated, cathepsin H was used in the experiments outlined. To confirm each protease was enzymatically active, protease activity control experiments were performed using a FRET-based fluorogenically labeled casein assay (Biovision #K781), according to the vendor's protocol. In brief, 1µM of each protease was added to a 50µL reaction mixture using the recommended concentration of control fluorogenic substrate in a buffer consisting of 50mM sodium acetate buffer at pH 4.5 and in the presence of 1mM EDTA and 2mM DTT. The assay was performed at 37ºC for 60 minutes and readings were taken every 2 minutes using Tecan Infinite M Plex plate reader.

Statistical analysis

Details of the statistical test used for each experiment is in figure legends along with n number and *p* value. All data is represented as mean ± SD. Statistical analysis was performed using GraphPad Prism 8 (GraphPad Software, La Jolla, California USA). A *P*-value < 0.05 was considered significant.

Cell culture, treatment, and lysis

Cell culture - SH-SY5Y human neuroblastoma cells were obtained from ATCC (CRL-2266) and maintained 1:1 EMEM/F12 media (ATCC #30-2003/Thermo #11765062) supplemented with 10% FBS and 1%

Penicillin-Streptomycin (Thermo #15140122). SH-SY5Y cells were differentiated by treating with 10µM all-trans retinoic acid (Sigma #R2625) for 6 days in EMEM/F12 media supplemented with 10% FBS and 1% Penicillin-Streptomycin, followed by 4 days of treatment with 50ng/mL of BDNF (Peprotech #450-02B) in EMEM/F12 media supplemented with only 1% Penicillin-Streptomycin. HEK293FT were maintained in high glucose DMEM media with 10%FBS and 1% Penicillin-Streptomycin. The WTC11 and isogenic progranulin KO iPSC cell lines [22,23] were gifted by Bruce Conklin's lab (Gladstone Institute, UCSF). For routine culture, iPSCs were plated in hESC matrigel (Corning #354277) coated plate with mTeSR plus (Stemcell Technologies #05825) and ROCKi (Stemcell Technologies #72304). iPSCs were maintained in mTeSR plus until confluent for lysate collection. Cells were washed with PBS -/- and dissociated with Accutase (Thermo Fisher Scientific #A1110501).

Cell treatments - For protease inhibition studies, day 10 post-differentiation SH-SY5Y cells were treated with 10µM E64D (Tocris Bioscience #4545), 20µM cathepsin L inhibitor II (Santa Cruz #sc-3132), and 15µM of CA074_methyl ester (Caymen Chemical Company #18469) or DMSO for 24 hours. For siRNA studies, day 10 post-differentiation SH-SY5Y cells were transfected according to the manufacturer's protocol using Oligofectamine (Invitrogen #12252011). Sixty hours post transfection, cells were collected for western blot analysis, as described below. siRNA scramble (Thermo Fisher #4390843), siRNA Legumain (Santa Cruz #sc-60930) were used. For overexpression studies, pCMV6 mammalian expressing vectors carrying the cDNA of AEP were ordered from Origene (#RC224975). XtremeGene HP (Sigma, # 06366236001) was used to transiently transfect HEK293FT cells for 24hours following the manufactures suggestions. The cells were then pelleted and prepared for western blotting as described below.

Cell Lysis - The cells were collected post-treatment and prepared for western blot analysis. Cells were washed once with PBS, trypsinized, and pelleted. The pellets were lysed in RIPA buffer (Fisher #89900) with protease and phosphatase inhibitors (Sigma #4693124001, #4906837001) and centrifuged at 15000 rpm at 4°C for 20 minutes. The supernatant containing the soluble proteins were transferred into a new tube. Estimated protein concentration with a Peirce BCA (Fisher # PI23225) protein assay kit following manufacturer's instructions. The nitrocellulose membrane was blocked with 5% milk (Fisher #NC9121673) or Odyssey buffer (Li-cor #927-50010) for 1-2hrs. The membranes were cut between 60-50kD and between 20-15kD to obtain PGRN and granulin-specific bands respectively and incubated with primary antibodies overnight [19]. Li-cor secondary antibodies at 1:5000 dilution was used and imaged using Odyssey CLx imager. Western blots were quantified using FIJI software.

Antibodies

Antibody generation - The following epitopes were used to generate the rabbit polyclonal anti-bodies:

paragranulin (p-Gran) -TRCPDGQFCPVACCLDPGGASYSCCRPLLD,

granulin F (Gran-F) - QCPDSQFECPDEST, and

granulin E (Gran-E) - ECGEGHFCHDNQTCCR.

Antibody validation – The sensitivity, specificity, and reproducibility of results of the novel p-Gran, Gran-F, and Gran-E antibodies were validated using a protocol similar to Bordeaux, et al. 2010 [24]. In brief, antibody specificity for each antigen was first measured by dot blot. For these experiments, 2.5µg of each granulin peptide was pipetted onto a nitrocellulose membrane defined into grids. Each antibody was incubated with the membrane overnight at 1:1000 dilution. Signals from the primary antibodies were amplified using species-specific antisera conjugated with horseradish peroxidase (Cell Signaling #7074) and detected with a chemiluminescent substrate detection system ECL and scanned the images with a densitometer. Following successful confirmation of antibody sensitivity, the specificity was evaluated via a peptide blocking experiment. Recombinant human progranulin was incubated with CTSL, a known PGRN protease, at pH 4.5 for 20 minutes at 37C as previously described. Samples were denatured and western blots were performed for peptide blocking analysis. Each primary antibody (p-Gran, Gran-F, Gran-E) was pre-incubated with its respective granulin peptide for 2 hours at room temperature with gentle mixing. Optimal primary antibody concentration was incubated with two different peptide amounts and on its own. Primary antibody to peptide ratio was determined by molarity at 10X, 100X, and no peptide. Following incubation, solutions were used to blot membranes overnight at 4C. Normal western blot procedure was completed as described.

Commercial antibodies - Anti-progranulin C-terminus (Thermo Fisher #40-3400, 1:200), Anti-granulin F (Sigma #HPA008763, 1:250), Anti-AEP (R&D #AF2199, 1:500), anti-Actin (Sigma #MAB1501R, 1:5000), and anti-FLAG (Sigma #F3165)

Human brain tissue lysis and analysis

Brain tissue was prepared as previously described in Salazar et al, 2015 [12]. Briefly, adjacent tissue blocks were fixed, embedded in paraffin wax, sectioned, stained for hematoxylin and eosin, and rated for astrogliosis (0–3 scale). Absent or low gliosis regions were selected with a score of 0-1, while high levels of gliosis regions with a score of 2-3. From this, we selected the middle frontal gyrus (MFG) with severe degeneration and inferior occipital cortex (IOC) with no degeneration for all assays. The same region was collected from control subjects. Brain tissue samples were weighed, diluted 25-fold with PBS (Thermo Fisher #14190250) and 1% triton-X (Millipore Sigma, #T9284), homogenized for 1 minute (pestle pellet motor) and sonicated for 5 rounds of 30 seconds on and 1 minute off (BioRuptor, Diagenode). The lysate was centrifuged at max for 20 minutes and the soluble supernatant was used for western blot assays. BCA was performed to determine protein concentration according to manufacturer's instructions. 25-50µg of total protein from each sample was loaded for western blot analysis. The nitrocellulose membrane was blocked with 5% milk (Fisher #NC9121673) or Odyssey buffer (Li-cor, #927-50010) for 1-2hrs. The membranes were cut between 60-50kD and between 20-15kD to obtain PGRN and granulin-specific bands respectively and incubated with primary antibodies overnight [19]. Li-cor secondary antibodies at 1:5000 dilution was used and imaged using Odyssey CLx imager. Western blots were quantified using FIJI software.

qPCR

Differentiated SH-SY5Y cells were pelleted and RNA was extracted using standard phenol:chloroform extraction techniques. 1µg of RNA was reverse transcribed to cDNA using Superscript III reverse transcription kit following manufacturer's protocol (Thermo Fisher #18080044), random primers (Thermo Fisher #48190011) and dNTPs (Sigma #11969064001). RT-qPCR was performed using TaqMan Fast Advanced Master Mix (Thermo Fisher #4444557) in a ABI Prism 7900HT Sequence Detection System (Applied Biosystems), with TaqMan FAM probes for human CTSB (Hs00947433_m1), CTSL (Hs009964650_m1), CTSK (Hs00166156_m1), CTSS (Hs00175407_m1), AEP/LGMN (Hs00271599_m1), CTSV (Hs00426731_m1), CTSE (Hs00157213_m1), CTSG (Hs01113415_g1) and the house keeping gene GAPDH (Hs02758991_g1) as a control. Four biological samples were analyzed, each with three technical replicates. mRNA levels of target genes were normalized to the mean of the house keeping gene GAPDH. Data is displayed as relative values compared to GAPDH.

Enzyme activity assays

AEP activity assay - AEP substrate Z-Ala-Ala-Asn-AMC (Bachem #I1865) was used to measure activity. 50mM sodium acetate buffer pH 5.5 with 2mM DTT, 1mM EDTA and 0.1% CHAPS was used as the assay buffer. 100µM of the substrate was used per reaction. The assay was performed at 37°C for 60 minutes and readings were taken every 2 minutes using Tecan Infinite M Plex plate reader. Activity was measured using excitation wavelength 380nm and emission wavelength 460nm. Assays were performed in triplicates for each sample.

CTSL activity assay - Biovision CTSL fluorometric assay kit (#K142) was used according to manufacturer's protocol with some modifications. Since CTSB can also cleave the assay substrate, the assay was performed with 1mM CTSB inhibitor (CA074_ME, Caymen Chemical Company #18469) to specifically assay CTSL activity. The assay was performed at 37°C for 60 minutes and reading were taken every 2 minutes using a Tecan Infinite M Plex plate reader. Activity was measured using excitation wavelength 400nm and emission wavelength 505nm. This assay was performed in triplicates for each sample.

Identification of AEP cleavage sites

In-gel Digestion - 400 ng of recombinant human progranulin (R&D #CF-2420) was incubated at 37°C for 60 minutes with recombinant human AEP (R&D #2199-CY) at pH 4.5. The cleavage was stopped by adding 7.5µl of NuPAGE 4X LDS (Fisher #NP0007), 3µl of 10X reducing agent (Fisher #NP0009) and denatured for 10 minutes at 70°C. The samples were run on precast NOVEX 4-12% Bis-Tris gels (Fisher #NP0321PK2) using MES buffer (Fisher #NP0002). The gel was fixed, and silver stained as described above. Protein bands were excised and digested in-gel with Endoproteinase Asp-N (Sigma-Aldrich #11054589001) as described previously [25,26]. The extracted digests were vacuum-evaporated, resuspended in 20µl of 0.1% formic acid, and desalted using C18 ZipTips (Millipore #ZTC18M096).

Mass Spectrometry - Asp-N peptides were analyzed by on-line LC-MS/MS using an Orbitrap Fusion Lumos (Thermo Scientific, San Jose, CA) coupled with a NanoAcquity M-Class UPLC system (Waters, Milford, MA). Peptides were separated over a 15cm x 75µm ID 3µm C18 EASY-Spray column (Thermo Scientific #ES800). Precursor ions were measured from 375 to 1500 m/z in the Orbitrap analyzer (resolution: 120,000; AGC: 4.0e5). Ions charged 2+ to 7+ were isolated in the quadrupole (selection window: 1.6 m/z units; dynamic exclusion window: 30 s; MIPS Peptide filter enabled), fragmented by HCD (Normalized Collision Energy: 30%) and measured in the Orbitrap (resolution: 30,000; AGC; 5.0e4). The cycle time was 3 seconds.

Peaklists were generated using PAVA (UCSF) and searched using Protein Prospector 5.23.0 against the SwissProt database (downloaded 9/6/2016) and a randomized concatenated database. Cleavage specificity was set as Asp-N/AEP (Asn-C) allowing 2 mis-cleavages. Carbamidomethylation of Cys was set as a constant modification and two of the following variable modifications were allowed per peptide: acetylation of protein N-termini, oxidation of Met, oxidation and acetylation of protein N-terminal Met, cyclization of N-terminal Gln, protein N-terminal Met loss, protein N-terminal Met loss and acetylation. Precursor mass tolerance was 20ppm and fragment mass tolerance was 30ppm. A subsequent search using the above parameters but limiting the search to the following accession numbers and a user defined PGRN amino acid sequence (the human sequence minus the first 18 amino acids and with a C-terminal 6xHis tag) was used for further analysis: B2FQP3 O08692 P02533 P02666 P02754 P02769 P04264 P28799 P35527 P35908 P85945 Q8PC00 Q91FI1 Q9R4J4 P07711 Q99538. Spectra containing AEP cleavage sites can be viewed in MS-Viewer with the search key "besr1qb6q4" or the following link: http://msviewer.ucsf.edu/prospector/cgi-bin/mssearch.cgi?report_title=MS-Viewer&search_key=besr1qb6q4&search_name=msviewer [27].

Results

Multiple lysosomal proteases digest human progranulin *in vitro*

Previous studies have identified CTSL and CTSB as intracellular PGRN proteases [17,19], however the endo-lysosomal compartment contains many other proteolytic enzymes that belong to distinctive classes with specific but overlapping peptide recognition motifs [28]. We wondered if ither other lysosomal enzymes also play a role in processing human PGRN. To identify which proteases can and cannot cleave PGRN, we performed extensive *in vitro* cleavage studies with commercially available recombinant human lysosomal enzymes. Although we were ultimately interested in which of the proteases can liberate individual granulin peptides, we first asked the question of which lysosomal proteases can *digest* or *break down* the full-length pro-protein in the inter-granulin linker regions (Fig. 1a). Since different proteases have distinct pH setpoints for optimal activity that can be substrate-dependent [28–30], we performed the study across a range of pH settings that represents the stepwise maturation of endo-lysosomal compartments.

Lysosomal proteases are classified based on the amino acid(s) in their active site. We first assayed the largest class of lysosomal proteases, the cysteine protease family [31,32]. As previously shown [17,19], the cysteine proteases CTSB and CTSL digested recombinant human PGRN (Fig. 1b). In addition, cathepsins K (CTSK), S (CTSS), V (CTSV) and asparagine endopeptidase (AEP) were also able to digest PGRN within 20 minutes. At an acidic pH of 4.5 or 5.5, CTSB, CTSL, CTSK, CTSS and CTSV digested most or all of full-length PGRN. AEP only modestly digested PGRN at pH 4.5 and 5.5 within the same time frame. CTSL and CTSV (also known as cathepsin L2), were the only cysteine protease that could digest PGRN at a pH as low as 3.4. Interestingly, CTSS, a lysosomal and secreted enzyme, is the only cysteine protease that can efficiently digest PGRN at both acidic and neutral pH, thereby making it a candidate enzyme to process both intracellular and extracellular PGRN [33]. In contrast, the cysteine cathepsins H (CTSH), C (CTSC), F (CSTF), O (CTSO) and X (CTSX) were unable to digest PGRN at any pH tested (Fig. 1b).

We next tested the aspartic acid family of acid hydrolases, which includes cathepsin E (CTSE), cathepsin D (CTSD) and napsin A. Cathepsin E (CTSE) is an endo-lysosomal aspartyl protease, highly expressed in immune cells such as microglia [34]. CTSE digested PGRN only at the most acidic pH of 3.4 (Fig. 1c). CTSD has been implicated in multiple neurodegenerative diseases and was previously demonstrated to associate with PGRN, which promotes CTSD maturation and activity [14,35–41]. One recent study reported that prolonged incubation (16 hours) of PGRN with CTSD at pH 3.5 can lead to PGRN cleavage, although low molecular weight granulin-sized bands were not observed [20]. Typically, proteases act on their substrates rapidly, within minutes. To determine if CTSD plays a role in degrading PGRN at more physiological time scales, we incubated mature CTSD with recombinant PGRN for 20 minutes. Under these *in vitro* conditions, CTSD did not degrade PGRN at any pH (Fig. 1c). To ensure that CTSD was indeed active, we tested its activity against a known substrate, BSA [41], in parallel with PGRN. At both pH 3.4 and 4.5, CTSD cleaved BSA but not PGRN (Fig. S1a). Thus, PGRN is likely not a physiological CTSD substrate or if it is, its activity is limited. Napsin A, which has been used as a biomarker of human cancers [42,43], did not degrade PGRN *in vitro* at any pH tested (Fig. 1c).

We then tested the final class of lysosomal proteases, the serine proteases. Pro-X-carboxypeptidase (PRCP) and cathepsin A (CTSA) were unable to digest PGRN at any pH tested (Fig. 1d). However, cathepsin G (CTSG), a lysosomal and secreted serine protease digested PGRN at pH 5.5 and 7.4. Therefore, CTSG, like CTSS, is a candidate protease to process both intracellular and extracellular PGRN.

To determine if the enzymes that do not cleave PGRN in our assay (CTSH, CTSC, CTSF, CTSO, CTSX, CTSD, napsin A, PRCP and CTSA) are active against another control substrate, we performed FRET-based cleavage assays with fluorogenically-tagged casein. The results confirm that all enzymes are active at pH 4.5 and can cleave this universal substrate, although with varied efficiencies (Fig. S1b).

Therefore, in total six cysteine (CTSB, CTSL, CTSK, CTSS, CTSV and AEP), one aspartyl (CTSE) and one serine protease (CTSG) rapidly digested full-length PGRN *in vitro* in a pH-dependent manner (Table 1). Since protease expression can be cell-specific and temporally regulated [28,44,45], these results

suggest that PGRN processing can be highly regulated, occuring in a protease-specific, pH-dependent manner and possibly both extracellularly and in multiple intracellular compartments.

PGRN undergoes pH-dependent processing into multi-granulin fragments and individual granulins *in vitro*

Progranulin is well-known to be a precursor protein for granulins, which are stress-responsive molecules with varying bioactivities [6–10]. Having established a subset of lysosomal proteases that can digest full-length PGRN, we next sought to understand which of these could proteolytically process PGRN into granulin-sized peptides. To do so, we generated custom anti-granulin antibodies raised against the N-terminal paragranulin (p-Gran), a centrally located peptide, granulin F (Gran-F) and C-terminal granulin E (Gran-E) (Fig. 2a and S2). We then analyzed the results of *in vitro* cleavage assays for lower molecular weight bands that represent MGFs or individual granulins. Consistent with our previous results, the lysosomal proteases that could not digest PGRN did not release any specific multi-granulin or individual granulin-sized fragments (Fig. S3). Given the large amount of data, we will first discuss the production of the N- and C-terminal granulins, followed by granulin F and finally the MGFs.

The N-terminal paragranulin can be released by a single cleavage after granulin p. Following incubation with CTSL and CTSK, and to a lesser extent in CTSS and CTSV, the anti-p-Gran antibody detected a <7kD band that likely represents this cleavage event that produces the paragranulin (Fig. 2b and S4). Similarly, the C-terminal granulin E can be released by a single cleavage after granulin D. Following incubation with CTSL, CTSK, and CTSV, and to a lesser extent CTSB, CTSS and CTSG, the anti-gran-E antibody detected a <10kD band that likely represents this cleavage and release of Gran-E (Fig. 2d and S4). Interestingly, the endo-lysosomal aspartyl protease CTSE also had the ability to process PGRN to release an ~12kD peptide containing granulin E, but only at pH 3.4, suggesting that CTSE may have a different cleavage pattern than other proteases (Fig. 2d).

Unlike paragranulin and granulin E, the release of granulin F requires two cleavages (after granulin G and before granulin B.)   Most individual proteases were inefficient at cleaving both of these specific linkers. CTSL, CTSK, CTSS and CTV robustly cleaved PGRN into MGFs containing granulin F, but inefficiently released individual granulin F, and only at pH 4.5 (Fig. 2c). AEP was a notable exception, as it could robustly release granulin F at pH 4.5 and 5.5. However, AEP was unable to liberate the N and C-terminal granulins (Fig. 2c and S4). These results suggest that different proteases cleave at different inter-granulin regions in PGRN in a pH-specific manner. This is summarized in Fig. S5.

Given that each intact PGRN molecule contains up to eight granulins and seven inter-granulin linkers, the potential number of different multi-granulin fragments could be quite high (up to 86 potential products). However, when we observed the actual pattern of multi-granulin fragments, we found that their molecular weights were largely similar across both cysteine and serine proteases (Fig. 2b-d). This suggests similar cleavage patterns for the different enzymes, albeit with different abundances. The notable exception to this pattern, once again, was AEP, which exhibited a distinctive pattern of

intermediate bands. Interesting differences in MGF production also emerged across pH, including shifts in the size of multi-granulin and individual granulin-sized bands (Fig. 2c-d, red asterisk).

To determine the efficiency of processing PGRN at different inter-granulin domains, we performed time-course experiments for the CTSL and CTSB (Fig. S6). Since both these enzymes digest almost all recombinant PGRN within 20mins (Fig. 1b and 2b), we decreased the enzyme concentration by 20-fold to 50nM and maintained the substrate concentration. Cleavage products were collected at the time points indicated and Western blotting performed using anti-p-Gran, Gran-F and Gran-E antibodies. The time-course data suggests that CTSL is highly efficient at releasing paragranulin and Gran-E from PGRN (Fig. S6a). CTSL can cleave the intergranulin linker between p-G as early as 2.5mins releasing paragranulin and between D-E within 10mins releasing granulin E. In contrast, CTSL does not liberate Gran-F even when incubated up to 60 mins at this concentration. This further confirms are results that CTSL can robustly process PGRN to release N-terminus paragranulin and C-terminus granulin E but is unable to liberate granulin F at the same concentration (Fig. 2). Interestingly, at this lower concentration, CTSB, another documented PGRN protease, is unable to process PGRN suggesting a much lower PGRN cleaving efficiency in comparison to CTSL (Fig. S6b). This data suggests that CTSL is more efficient at processing PGRN than CTSB.

In summary, our results demonstrate that eight lysosomal proteases are capable of digesting full-length human PGRN *in vitro*. Moreover, these findings demonstrate that each of these enzymes can cleave PGRN into one or more individual granulin (Fig. S5b). When tested in isolation, the majority of cysteine, aspartyl and serine proteases tended to liberate N and/or C-terminal granulins. In contrast, AEP was unable to liberate the N- and/or C-terminal granulins but robustly liberated granulin F, present in the center of the pro-protein. Furthermore, one cysteine (CTSS) and one serine protease (CTSG) processed PGRN into granulins at neutral pH (7.4) while an aspartyl protease (CTSE) could only process PGRN at highly acidic pH (3.4).

Asparagine endopeptidase is a PGRN protease that liberates granulin F

To assess the specificity of our custom anti-granulin antibodies, we used a pair of previously published, isogenic wild-type and progranulin knockout (KO) iPSC cell lines [22,23]. Unlike for recombinant progranulin or the commercially available Invitrogen and Sigma anti-progranulin antibodies, the anti-p-gran, gran-F and Gran-E antibodies did not robustly recognize full-length PGRN from whole cell lysates (Fig. S7a). This may be due to coverage of the epitope by glycosylation or another post-translational modification. Our anti-Gran-F antibody and the Sigma antibody both recognized a granulin-sized band, which according to a recent study of all available commercial PGRN antibodies [19], is likely to be granulin F. With all of the antibodies, comparison of *Pgrn* WT and KO cells revealed many non-specific bands. Given these findings and the limited quantities of the custom antibodies available, we chose to utilize the Invitrogen and the Sigma antibodies to detect full-length endogenous PGRN and granulin F, respectively, in cell-based studies.

To study the processing of PGRN *in vivo* in cells, we chose SH-SY5Y cells for their ability to be terminally differentiated into neuron-like cells. These cells produce detectable amounts of both endogenous PGRN and granulin F (Fig. 3a). We first determined the expression profile of PGRN-cleaving proteases by qPCR analysis. We found that the lysosomal proteases CTSB, CTSL, CTSK, CTSS, AEP and CTSE were expressed in differentiated SH-SY5Y cells, but CTSV and CTSG were not detected (Fig. S8).

Since AEP is the only protease that robustly liberated granulin F *in vitro*, and granulin F is the only granulin that can be reliably detected from cell lysates [19], we next sought to further validate AEP as a PGRN protease in these cells. To determine if AEP cleaves PGRN endogenously in terminally differentiated SH-SY5Y cells, we performed siRNA knock down of AEP and assessed the levels of endogenous PGRN and granulin F in terminally differentiated SH-SY5Y cells. Consistent with our *in vitro* results, a modest knock down of AEP (~25%) resulted in a significant decrease in the levels of granulin F compared to scramble-treated controls (Fig. 3a). To further validate our results, we transiently overexpressed FLAG-tagged AEP (Fig. 3b). These studies were performed HEK293FT cells for ease of expression and transfection. Overexpression of AEP led to significantly increased in granulin F levels (Fig. 3b).

To determine the specific cleavage sites of AEP, we incubated recombinant human PGRN with and without AEP for 60 minutes at pH 4.5. Bands corresponding to full-length PGRN, multi-granulin bands, and granulin-sized bands were observed by silver staining (Fig. S9a). All bands underwent LC-MS/MS to determine AEP cleavage sites. Consistent with its activity as a protease that cleaves after asparagine residues, we identified three sites for AEP cleavage within three inter-granulin linkers (G-F, F-B, B-A) that would result in the liberation of granulins F and B from PGRN (Fig. 4, S9b-S9e).

Granulins F levels are increased in the degenerating regions of the brains from FTLD-TDP-*Pgrn* patients

PGRN haploinsufficiency predisposes to FTLD-TDP. Interestingly, in *C. elegans*, the processing of progranulin to granulins increases with age [46]. Further, the presence of an MGF containing granulin E is decreased in FTLD-TDP [12]. However, whether PGRN processing into granulin F is affected in FTLD, an age-related disorder, is unclear. To assess whether PGRN processing is altered in FTLD, we measured granulin F levels from brain samples of control individuals or those with FTLD due to *Pgrn* mutations (FTLD-TDP-*Pgrn*). As previously described [12], we examined a brain region affected in FTLD (middle frontal gyrus, MFG, defined as gliosis score of 3) as well as an unaffected region (inferior occipital cortex, IOC, defined as gliosis score of 0-1) from both groups. Characteristics of subjects are shown in Table 2.

Similar to previous studies [19,47], the FTLD-TDP-*Pgrn* group exhibited significantly less full-length PGRN protein in both unaffected and affected brain regions compared to control subjects (Fig. 5a and 5b). However, granulin F was increased relative to controls in the diseased MFG region (Fig. 5a-c). Notably, this difference was present despite the relatively younger ages of the control cases (Fig. S10).

Since AEP was the only enzyme that could robustly liberate granulin F in our *in vitro* assays and affected the levels of granulin F in cells (Fig. 2 and 3), we quantified the activity of AEP in both regions of the brain. Activity assays revealed a significant increase in AEP activity in disease-affected MFG compared to non-affected IOC from the same subjects, as well as a trend toward increased activity (p=0.07) between control and FTLD-TDP-*Pgrn* MFG (Fig 5d). Furthermore, a similar trend towards and increased level of both immature and mature AEP was seen in the degenerating MFG region compared to the non-affected IOC regions of FTLD-TDP-*Pgrn* samples (Fig. S11c and 11d). To determine if the change in levels and activity AEP was also seen for other PGRN proteases, we assayed the activity of CTSL, a previously known PGRN protease. Interestingly, there was no significant change to CTSL activity in either regions across groups, suggesting differential effects on lysosomal enzymes in FTLD (Fig. 5e).

These data suggest that increased AEP activity in the degenerating MFG region may alter PGRN processing in a way that leads to an increase in production of granulin F in that region. We were unable to detect other granulin peptides but had previously shown in both FTLD-TDP patients negative for *Pgrn* mutations and Alzheimer's disease brain that a multi-granulin fragment containing granulin E was also increased in a diseased brain region [12]. Thus, it may be that either these neurodegenerative diseases or the gliosis associated with them leads to overall increased processing of PGRN.

Discussion

This study sought to better understand all aspects of PGRN cleavage into granulins, from the proteases involved and pH-dependence of cleavage to the MGFs/granulins produced and relevance to human disease. The normal functions of PGRN as an activator of CTSD are slowly being elucidated [14, 46]. However, granulins are less well-understood. Since full-length, partially cleaved and granulins are all bioactive [14, 35], a complete and nuanced understanding of their production and levels will likely be critical to understanding normal, balanced PGRN function and how this changes with age and disease. We have shown that in addition to CTSL and CTSB, multiple proteases can process PGRN and liberate granulins, and all of these proteases act in a pH-dependent manner. Additionally, these proteases have differential expressions in cells and tissues. CTSB, CTSL and AEP are expressed in all cells and tissues including the brain, however CTSS, CTSK, CTSV, CTSE and CTSG show cell- and tissue-specific expression [2,32,44,45]. This suggests that PGRN processing may be regulated in a cell-type specific manner and future studies in cells that endogenously express these proteases may help better understand their roles.

Although our *in vitro* assays identified the ability of individual proteases to cleave PGRN into granulins, we recognize several limitations to these types of assays. First, they lack key PGRN binding partners, such as prosaposin and potential co-factors that can modulate protease activity, such as peptide inhibitors like cystatins and aspartins. Secondly, PGRN in lysosomes will likely be simultaneously cleaved by multiple proteases that also interact with one another [48], which is not simulated in this approach. However, to gain clarity as to the complement of lysosomal proteases that are able to cleave PGRN, this study is the first and most comprehensive of its kind. The ability to differentiate between types

of MGFs, pH optima, and relative efficiency of protease cleavage of PGRN are other advantages to our approach.

The experiments in terminally differentiated SH-SY5Y cells revealed that individual granulins may be produced by serial or stepwise cleavage of PGRN by multiple proteases. These results suggest that cysteine proteases such as CTSB and/or CTSL process full-length PGRN to mainly produce multi-granulin fragments that contain granulin F and to a lesser extent individual granulin F (similar to our *in vitro* assay), while AEP may act on one or more of these fragments to produce individual granulin F. It is therefore possible that the modest reduction in granulin F levels seen upon dual inhibition of CTSB and CTSL is due to reduced availability of multi-granulin fragments for AEP to process. To our knowledge, this is the first study to identify cleavage sites in the inter-granulin linkers required to liberate granulin F. Earlier studies in human primary cell cultures have also referred to a potential multi-granulin fragment likely containing granulin F[49,50]. Future studies, including studies in mice, on these multi-granulin fragments will be essential to tease out the complex regulation of PGRN processing.

While we and others have shown alterations in granulin levels in FTLD-TDP [12,19], this study is the first study to implicate a change in a specific protease, AEP. To our surprise, these results also demonstrated elevated granulin F levels in areas of severe neurodegeneration in human GRN-FTD cases. Previously, Holler et al, 2017, demonstrated a reduction in certain granulins in brain, however, the severity of degeneration and astrogliosis within these regions was not assessed [19]. Since these degenerating regions are characterized by neuronal loss and infiltration of inflammatory astrocytes and microglia, the latter of which expresses high levels of AEP [45], it is possible that glial cells, such as astrocytes or microglia, are responsible for the increased granulin F. Moreover, since PGRN is also a secreted protein, we cannot yet differentiate the cell autonomous and cell non-autonomous contributions of PGRN processing in disease. Whether the increased granulin F contributes to or results from FTLD pathophysiology also remains to be seen. AEP has previously been reported to cleave aggregate-forming proteins, such as amyloid precursor protein (APP), microtubule associated protein tau (MAPT) and TAR-DNA binding protein 43 (TDP43) and is also implicated in an FTLD-related disorder, amyotrophic lateral sclerosis (ALS) [32,51–54]. Interestingly, AEP is dysregulated and activated during aging, and AEP activity is increased in regions of degeneration in AD human brain and mouse models suggesting that PGRN processing and granulin F production may be altered in other neurodegenerative diseases as well[52]. If future studies implicate a causal role for granulin F in FTLD and other diseases, targeting AEP to decrease the levels of granulin F in the degenerating regions of the brain may be neuroprotective.

In summary, our study suggests that PGRN processing into granulins undergoes multiple levels of regulation, including protease-specific cleavage sites in the various inter-granulin linkers and differential cleavage based on pH setpoints, which may reflect activity in different endo-lysosomal compartments. Still to be explored are cell-type and temporal regulation of PGRN cleavage. Given the highly evolutionarily conserved presence of PGRN and granulins, as well as the gene mutations associated with disease, intricate regulation indicates that PGRN and granulin levels are important for maintaining cellular homeostasis and function. Our studies have helped identify multiple players that contribute to

this homeostasis, providing new avenues to regulate the levels of granulins in disease and placing the broad and contrasting roles of granulins into perspective.

Conclusion

This study comprehensively identifies a suite of endo-lysosomal proteases that can process full-length PGRN into multi-granulin and single granulin fragments. These proteases have strikingly specific cleavage patterns and optimal pH settings. The complexity of PGRN cleavage could confer multiple layers of cell-type and environmentally responsive regulation upon PGRN processing that can be altered with age and disease. As full-length, multi-granulin and single granulin fragments likely have different biological activities, these findings are highly relevant in understanding the consequences of progranulin replacement therapies and could be leveraged to promote neuronal health through inhibition of specific PGRN proteases.

Abbreviations

PGRN - Progranulin

Gran-F – granulin F

p-Gran – paragranulin

Gran-E – granulin E

CTSB – Cathepsin B

CTSL – Cathepsin L

CTSK – Cathepsin K

CTSS – Cathepsin S

CTSV – Cathepsin V

AEP – Asparagine endopeptidase

CTSH – Cathepsin H

CTSX – Cathepsin X

CTSC – Cathepsin C

CTSD – Cathepsin D

CTSE – Cathepsin E

CTSF – Cathepsin F

CTSO – Cathepsin O

CTSG – Cathepsin G

PRCP – Pro-X carboxypeptidase

CTSA – Cathepsin A

FTLD-TDP-*Pgrn* – Frontotemporal lobar degeneration leading to TDP-43 positive inclusions caused by progranulin haploinsufficiency

AD – Alzheimer's disease

MAPT -microtubule associated protein Tau

IOC – inferior occipital cortex

MFG – middle frontal gyrus

Declarations

Ethical Approval and consent to participate

Not Applicable

Consent for publication

All authors have reviewed the final manuscript and consent to publication.

Availability of data and materials

All data generated or analysed during this study are included in this published article [and its supplementary information files].

Completing interests

The authors declare they have no completing interests.

Authors' contributions

S.M and A.W.K conceived the project. S.M designed all experiments. P.J.S. and E.C.C. performed many of the *in vitro* western blots and silver stain experiments as well as the non-cleaving enzyme activity assays. A.P. assisted in knock down and over-expression studies. K.H.L, J.C.M and A.B. performed LC/MS/MS. A.M performed the dot blot analysis. W.W.S. and B.L.M. provided the brain samples. A.R.A performed the peptide blocking assay, iPSCs and brain western blots. S.M performed all other experiments and analyzed all the data. S.M, P.J.S. and A.W.K composed the manuscript. All authors read and approved the final manuscript.

Acknowledgements

Authors' information

Not Applicable

References

REFERENCES

1. Kao AW, McKay A, Singh PP, Brunet A, Huang EJ. Progranulin, lysosomal regulation and neurodegenerative disease. Nat Rev Neurosci. 2017;18:325–33.
2. Palfree RGE, Bennett HPJ, Bateman A. The Evolution of the Secreted Regulatory Protein Progranulin. Plos One. 2015;10:e0133749.
3. Baker M, Mackenzie IR, Pickering-Brown SM, Gass J, Rademakers R, Lindholm C, et al. Mutations in progranulin cause tau-negative frontotemporal dementia linked to chromosome 17. Nature. 2006;442:916–9.
4. Cruts M, Gijselinck I, Zee J van der, Engelborghs S, Wils H, Pirici D, et al. Null mutations in progranulin cause ubiquitin-positive frontotemporal dementia linked to chromosome 17q21. Nature. 2006;442:920–4.
5. Smith KR, Damiano J, Franceschetti S, Carpenter S, Canafoglia L, Morbin M, et al. Strikingly Different Clinicopathological Phenotypes Determined by Progranulin-Mutation Dosage. Am J Hum Genetics.

2012;90:1102–7.

6. Kessenbrock K, Fröhlich L, Sixt M, Lämmermann T, Pfister H, Bateman A, et al. Proteinase 3 and neutrophil elastase enhance inflammation in mice by inactivating antiinflammatory progranulin. J Clin Invest. 2008;118:2438–47.

7. Tang W, Lu Y, Tian Q-Y, Zhang Y, Guo F-J, Liu G-Y, et al. The Growth Factor Progranulin Binds to TNF Receptors and Is Therapeutic Against Inflammatory Arthritis in Mice. Science. 2011;332:478–84.

8. Zhu J, Nathan C, Jin W, Sim D, Ashcroft GS, Wahl SM, et al. Conversion of Proepithelin to Epithelins Roles of SLPI and Elastase in Host Defense and Wound Repair. Cell. 2002;111:867–78.

9. Tolkatchev D, Malik S, Vinogradova A, Wang P, Chen Z, Xu P, et al. Structure dissection of human progranulin identifies well-folded granulin/epithelin modules with unique functional activities. Protein Sci. 2008;17:711–24.

10. Plowman GD, Green JM, Neubauer MG, Buckley SD, McDonald VL, Todaro GJ, Shoyab M. The epithelin precursor encodes two proteins with opposing activities on epithelial cell growth. J Biol Chem. 1992;267:13073-8.

11. Bhandari V, Palfree RG, Bateman A. Isolation and sequence of the granulin precursor cDNA from human bone marrow reveals tandem cysteine-rich granulin domains. Proc National Acad Sci. 1992;89:1715–9.

12. Salazar DA, Butler VJ, Argouarch AR, Hsu T-Y, Mason A, Nakamura A, et al. The Progranulin Cleavage Products, Granulins, Exacerbate TDP-43 Toxicity and Increase TDP-43 Levels. J Neurosci. 2015;35:9315–28.

13. Thurner L, Fadle N, Regitz E, Kemele M, Klemm P, Zaks M, et al. The molecular basis for development of proinflammatory autoantibodies to progranulin. J Autoimmun. 2015;61:17–28.

14. Butler VJ, Cortopassi WA, Gururaj S, Wang AL, Pierce OM, Jacobson MP, et al. Multi-Granulin Domain Peptides Bind to Pro-Cathepsin D and Stimulate Its Enzymatic Activity More Effectively Than Progranulin in Vitro. Biochemistry-us. 2019;58:2670–4.

15. Suh H-S, Choi N, Tarassishin L, Lee SC. Regulation of Progranulin Expression in Human Microglia and Proteolysis of Progranulin by Matrix Metalloproteinase-12 (MMP-12). Plos One. 2012;7:e35115.

16. Hu F, Padukkavidana T, Vægter CB, Brady OA, Zheng Y, Mackenzie IR, et al. Sortilin-Mediated Endocytosis Determines Levels of the Frontotemporal Dementia Protein, Progranulin. Neuron. 2010;68:654–67.

17. Lee CW, Stankowski JN, Chew J, Cook CN, Lam Y-W, Almeida S, et al. The lysosomal protein cathepsin L is a progranulin protease. Mol Neurodegener. 2017;12:55.

18. Tanaka Y, Matsuwaki T, Yamanouchi K, Nishihara M. Increased lysosomal biogenesis in activated microglia and exacerbated neuronal damage after traumatic brain injury in progranulin-deficient mice. Neuroscience. 2013;250:8–19.

19. Holler CJ, Taylor G, Deng Q, Kukar T. Intracellular Proteolysis of Progranulin Generates Stable, Lysosomal Granulins that Are Haploinsufficient in Patients with Frontotemporal Dementia Caused by GRN Mutations. Eneuro. 2017;4:ENEURO.0100-17.2017.

20. Zhou X, Paushter DH, Feng T, Sun L, Reinheckel T, Hu F. Lysosomal processing of progranulin. Mol Neurodegener. 2017;12:62.

21. Nguyen AD, Nguyen TA, Cenik B, Yu G, Herz J, Walther TC, et al. Secreted Progranulin Is a Homodimer and Is Not a Component of High Density Lipoproteins (HDL). J Biol Chem. 2013;288:8627–35.

22. Miyaoka Y, Chan AH, Judge LM, Yoo J, Huang M, Nguyen TD, et al. Isolation of single-base genome-edited human iPS cells without antibiotic selection. Nat Methods. 2014;11:291–3.

23. Narendra DP, Guillermier C, Gyngard F, Huang X, Ward ME, Steinhauser ML. Coupling APEX labeling to imaging mass spectrometry of single organelles reveals heterogeneity in lysosomal protein turnover. J Cell Biology. 2020;219.

24. Bordeaux J, Welsh AW, Agarwal S, Killiam E, Baquero MT, Hanna JA, et al. Antibody validation. Biotechniques. 2010;48:197–209.

25. Rosenfeld J, Capdevielle J, Guillemot JC, Ferrara P. In-gel digestion of proteins for internal sequence analysis after one- or two-dimensional gel electrophoresis. Anal Biochem. 1992;203:173–9.

26. Hellman U, Wernstedt C, Gonez J, Heldin CH. Improvement of an "In-Gel" Digestion Procedure for the Micropreparation of Internal Protein Fragments for Amino Acid Sequencing. Anal Biochem. 1995;224:451–5.

27. Baker PR, Chalkley RJ. MS-Viewer: A Web-based Spectral Viewer for Proteomics Results. Mol Cell Proteomics. 2014;13:1392–6.

28. Turk V, Stoka V, Vasiljeva O, Renko M, Sun T, Turk B, Turk D. Cysteine cathepsins: from structure, function and regulation to new frontiers. Biochim Biophys Acta 2012;1824:68–88.

29. Banay-Schwartz M, Bracco F, Dahl D, DeGuzman T, Turk V, Lajtha A. The pH dependence of breakdown of various purified brain proteins by cathepsin D preparations. Neurochem Int. 1985;7:607–14.

30. Turk B, Dolenc I, Lenarčič B, Križaj I, Turk V, Bieth JG, et al. Acidic pH as a physiological regulator of human cathepsin L activity. Eur J Biochem. 1999;259:926–32.

31. Rossi A, Deveraux Q, Turk B, Sali A. Comprehensive search for cysteine cathepsins in the human genome. Biol Chem. 2004;385:363–72.

32. Dall E, Brandstetter H. Structure and function of legumain in health and disease. Biochimie. 2016;122:126–50.

33. Jordans S, Jenko-Kokalj S, Kühl NM, Tedelind S, Sendt W, Brömme D, et al. Monitoring compartment-specific substrate cleavage by cathepsins B, K, L, and S at physiological pH and redox conditions. Bmc Biochem. 2009;10:23.

34. Zaidi N, Kalbacher H. Cathepsin E: A mini review. Biochem Bioph Res Co. 2008;367:517–22.

35. Butler VJ, Cortopassi WA, Argouarch AR, Ivry SL, Craik CS, Jacobson MP, et al. Progranulin Stimulates the in vitro Maturation of pro-Cathepsin D at Acidic pH. J Mol Biol. 2019;431:1038–47.

36. Stoka V, Turk V, Turk B. Lysosomal cathepsins and their regulation in aging and neurodegeneration. Ageing Res Rev. 2016;32:22–37.

37. Valdez C, Wong YC, Schwake M, Bu G, Wszolek ZK, Krainc D. Progranulin-mediated deficiency of cathepsin D results in FTD and NCL-like phenotypes in neurons derived from FTD patients. Hum Mol Genet. 2017;26:4861–72.

38. Zhou X, Paushter DH, Feng T, Pardon CM, Mendoza CS, Hu F. Regulation of cathepsin D activity by the FTLD protein progranulin. Acta Neuropathol. 2017;134:151–3.

39. Beel S, Moisse M, Damme M, Muynck LD, Robberecht W, Bosch LVD, et al. Progranulin functions as a cathepsin D chaperone to stimulate axonal outgrowth in vivo. Hum Mol Genet. 2017;26:2850–63.

40. Ward ME, Chen R, Huang H-Y, Ludwig C, Telpoukhovskaia M, Taubes A, et al. Individuals with progranulin haploinsufficiency exhibit features of neuronal ceroid lipofuscinosis. Sci Transl Med. 2017;9:eaah5642.

41. Sun H, Lou X, Shan Q, Zhang J, Zhu X, Zhang J, et al. Proteolytic Characteristics of Cathepsin D Related to the Recognition and Cleavage of Its Target Proteins. Plos One. 2013;8:e65733.

42. Yamashita Y, Nagasaka T, Naiki-Ito A, Sato S, Suzuki S, Toyokuni S, et al. Napsin A is a specific marker for ovarian clear cell adenocarcinoma. Modern Pathol. 2015;28:111–7.

43. Uchida A, Samukawa T, Kumamoto T, Ohshige M, Hatanaka K, Nakamura Y, et al. Napsin A levels in epithelial lining fluid as a diagnostic biomarker of primary lung adenocarcinoma. Bmc Pulm Med. 2017;17:195.

44. Korkmaz B, Horwitz MS, Jenne DE, Gauthier F. Neutrophil Elastase, Proteinase 3, and Cathepsin G as Therapeutic Targets in Human Diseases. Pharmacol Rev. 2010;62:726–59.

45. Zhang Y, Sloan SA, Clarke LE, Caneda C, Plaza CA, Blumenthal PD, et al. Purification and Characterization of Progenitor and Mature Human Astrocytes Reveals Transcriptional and Functional Differences with Mouse. Neuron. 2016;89:37–53.

46. Butler VJ, Gao F, Corrales CI, Cortopassi WA, Caballero B, Vohra M, et al. Age- and stress-associated C. elegans granulins impair lysosomal function and induce a compensatory HLH-30/TFEB transcriptional response. Plos Genet. 2019;15:e1008295.

47. Chen-Plotkin AS, Xiao J, Geser F, Martinez-Lage M, Grossman M, Unger T, et al. Brain progranulin expression in GRN-associated frontotemporal lobar degeneration. Acta Neuropathol. 2009;119:111.

48. Olson OC, Joyce JA. Cysteine cathepsin proteases: regulators of cancer progression and therapeutic response. Nat Rev Cancer. 2015;15:712–29.

49. Alquezar C, Esteras N, Encarnación A de la, Moreno F, Munain AL de, Martín-Requero Á. Increasing progranulin levels and blockade of the ERK1/2 pathway: Upstream and downstream strategies for the treatment of progranulin deficient frontotemporal dementia. Eur Neuropsychopharm. 2015;25:386–403.

50. Encarnación A de la, Alquézar C, Esteras N, Martín-Requero Á. Progranulin Deficiency Reduces CDK4/6/pRb Activation and Survival of Human Neuroblastoma SH-SY5Y Cells. Mol Neurobiol. 2015;52:1714–25.

51. Chen J-M, Dando PM, Rawlings ND, Brown MA, Young NE, Stevens RA, et al. Cloning, Isolation, and Characterization of Mammalian Legumain, an Asparaginyl Endopeptidase. J Biol Chem.

1997;272:8090–8.

52. Rosenmann H. Asparagine endopeptidase cleaves tau and promotes neurodegeneration. Nat Med. 2014;20:1236–8.

53. Zhang Z, Song M, Liu X, Kang SS, Kwon I-S, Duong DM, et al. Cleavage of tau by asparagine endopeptidase mediates the neurofibrillary pathology in Alzheimer's disease. Nat Med. 2014;20:1254–62.

54. Herskowitz JH, Gozal YM, Duong DM, Dammer EB, Gearing M, Ye K, et al. Asparaginyl endopeptidase cleaves TDP-43 in brain. Proteomics. 2012;12:2455–63.

55. Hawdon JM, Emmons SW, Jacobson LA. Regulation of proteinase levels in the nematode Caenorhabditis elegans. Preferential depression by acute or chronic starvation. Biochem J. 1989;264:161–5.

Tables

Due to technical limitations, tables 1-2 are only available as downloads in the supplemental files section.

Table 1. PGRN cleavage by lysosomal proteases *in vitro*

Summary of whether the enzymes tested could cleave progranulin (PGRN) or not along with the potential compartment it may cleave PGRN depending on the pH it processed progranulin *in vitro*. En, endosomes; Ly, lysosomes; Ex, extracellular.

Table 2. Clinical Information for control and FTLD-TDP-*Pgrn* subjects

Clinical information for the control and FTLD-TDP-*Pgrn* subjects. PMI, post-mortem interval; IOC, inferior occipital cortex; MFG, middle frontal gyrus.

Supplementary Figure Legends

Figure S1. Enzymes that do not cleave PGRN are active

a, 1μM of mature CTSD was incubated with 400ng recombinant human PGRN or 400ng BSA at the indicated pH. The incubation was stopped after 60 minutes, and reaction contents were subjected to Coomassie staining. Bands correlate to proteins indicated on the right. BSA was used as a control for CTSD activity. At lower pH of 3.4, CTSD self-digest leading to a decreased level of mature CTSD compared to pH 4.5 [55]. **b,** FRET-based enzyme activity assay at pH 4.5 was performed on all enzymes that do not cleave PGRN. The values obtained were normalized to timepoint 0 and plotted relative to activity. All enzymes show activity against the optimized FRET peptides compared to substrate only control.

Figure S2. Antibody validation for individual granulin peptides

a, Dot blots confirming the specificity of each in-house antibody towards the granulin peptide. 2.5µg of each peptide was used with each antibody (1:1000 dilution). Paragranulin, p-Gran; granulin G, Gran-G; granulin F, Gran-F; granulin B, Gran-B; granulin A, Gran-A; granulin C, Gran-C; granulin D, Gran-D; granulin E, Gran-E. **b,** Peptide blocking experiment to demonstrate antibody specificity. 400ng of rhPGRN was incubated with 1uM CTSL for 20mins. The antibody was incubated with the respective peptide (2 ratios) and then incubated with the membrane overnight. Increase in peptide concentrations show a decrease in the bands of each antibody tested.

Figure S3. Lysosomal proteases unable to digest PGRN *in vitro*

Full western blot images of the proteases that do not cleave PGRN. 1µM of each enzyme was incubated with 400ng of PGRN for 20 minutes. C-terminal Gran-E antibody or anti-PGRN (Invitrogen) antibody was used to assess the results of the *in vitro* assay. **a**, Cysteine proteases Cathepsins C (CTSC), H (CTSH), X (CTSX), O (CTSO) and F (CTSF). **b,** Aspartyl proteases cathepsin D (CTSD) and Napsin A. **c**, Serine protease Pro-X carboxypeptidase (PRCP) and Cathepsin A (CTSA). The lower molecular weight bands (indicated by *) correspond to the enzyme.

Figure S4. PGRN processing by lysosomal proteases *in vitro* at pH 6.5

1µM of each enzyme was incubated with 400 ng of PGRN for 20 minutes at pH 6.5. Anti-p-Gran, anti-Gran-F, and anti- Gran-E antibodies were used to assess the results of the *in vitro* assay. cathepsin B (CTSV), cathepsin L (CTSL), cathepsin K (CTSK), cathepsin S (CTSS), cathepsin V (CTSV), asparagine endopeptidase (AEP), cathepsin G (CTSG), paragranulin (p-Gran), granulin F (Gran-F), granulin E (Gran-E).

Figure S5. Summary of PGRN processing into granulins by multiple proteases

Summary of the results of the *in vitro* assays. **a**, Processing of PGRN to granulins by different proteases is dependent on pH. The range of cleavage is represented in greyscale with no cleavage in white and complete cleavage in black. The range takes into account the amount of full-length PGRN processed into multi-granulin fragments and individual granulins within 20 minutes. **b**, Represented is the ability of each enzyme to liberate individual paragranulin (p) in red, granulin F (F) in green, and granulin E (E) in blue. The protease classes are also indicated. CTSE, cathepsin E; CTSV, cathepsin V; CTSL, cathepsin L; CTSB, cathepsin B; CTSK, cathepsin K; AEP, asparagine endopeptidase; CTSG, cathepsin G; CTSS, cathepsin S.

Figure S6. CTSL is highly efficient at liberating paragranulin and granulin E from PGRN

A time course analysis to determine efficiency of cleavage. 400ng of recombinant human PGRN was incubated with 50nM of enzyme for the time points indicated. P-Gran, Gran-F and Gran-E antibodies were used to assess the results of the assay. PGRN, progranulin; CTSL, cathepsin L; CTSB, cathepsin B.

Figure S7. Antibody specificity to detect both PGRN and granulin sized bands in wild-type and PGRN knock out iPSC cell lysates

a, Lysates from isogenic WTC11 and *Pgrn* KO iPSCs were probed with custom anti-granulin antibodies. **b**, Commercial antibodies from Invitrogen and Sigma were tested on the the same iPSC cell lines.

Figure S8. Expression profile of the PGRN proteases in differentiated SH-SY5Y cells

qPCR analysis to assess the expression of candidate PGRN proteases in differentiated SH-SY5Y cells. The graph represents the mean expression value of each enzyme normalized to GAPDH. The absolute mean values are noted for each sample. All enzymes were run in triplicates with N=4 biological replicates.

Figure S9. PGRN is processed by AEP to liberate individual granulins F and B

Recombinant human PGRN was incubated with and without AEP for 1 hour at pH 4.5. The reaction was stopped, and the cleavage bands were separated by SDS-PAGE. **a,** Multiple cleavage bands and individual granulin sized bands can be visualized upon silver stain. **b-e,** Bands were cut and digested for mass spectrometry to identify the cleavage sites (also see Fig. 4c). Identified peptides are annotated with observed fragment ions. Previous and next amino acids are in () and carbamidomethylated Cys are colored red. The precursor mass of each peptide is as follows: b, 428.5229 m/z; c, 847.8607 m/z; d, 639.3205 m/z; e, 478.9133 m/z.

Figure S10. Progranulin and granulin F levels do not correlate with ages of subjects

The levels of PGRN and Gran-F, normalized to actin, is plotted alongside the age of that subject and the region of the brain.

Figure S11. AEP levels tend to increase in degenerating brain regions of FTLD-TDP-*Pgrn* patients

a, Western blot analysis of endogenous immature (pro AEP) and mature AEP levels. **b**, Quantification of pro and mature AEP levels in both IOC and MFG regions in FTLD-TDP-*Pgrn* patients compared to the same regions in control subjects. Multiple two-tailed unpaired t-test was performed between the different groups. No significant difference was observed within each region. **c,** Western blots of endogenous Pro and mature AEP in IOC and MFG brain regions of FTLD-TDP-*Pgrn* subjects. **d**, We observed an increasing trend in the levels of both pro and mature-AEP in the degenerating MFG region compared to the non-degenerating IOC region from the same FTLD brain. n=5. Multiple two-tailed student t-test was performed between the groups. IOC, inferior occipital cortex; MFG, middle frontal gyrus; AEP, asparagine endopeptidase. Sample numbers correspond to Table 2

Figures

Figure 1. Progranulin can be digested by multiple lysosomal proteases *in vitro*
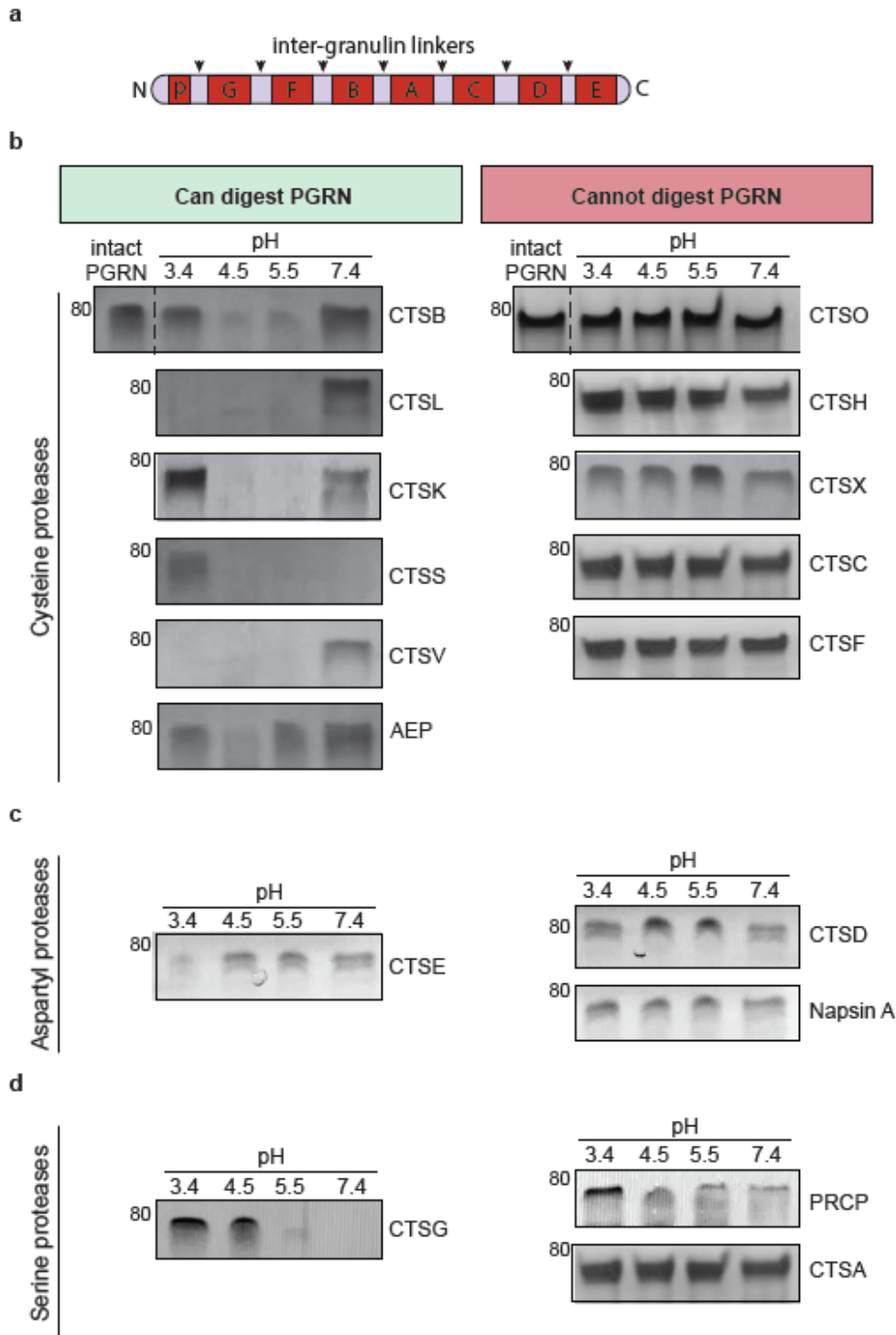
Figure 1

Progranulin can be digested by multiple lysosomal proteases in vitro a, Schematic representation of progranulin (PGRN) protein. Black arrows indicate inter-granulin linkers, individual granulins named granulins A-G (~7kD each) and paragranulin (p) (~3.5kD) are annotated. b, c, d, 1μM of each enzyme was incubated with 400ng of recombinant human PGRN at the indicated pH for 20 minutes. The proteins were

silver stained (shown in greyscale) to assess the presence or absence of PGRN at every condition. All assays were repeated n=3 times.

Figure 2. PGRN undergoes pH dependent processing into multi-granulin fragments and individual granulins *in vitro*
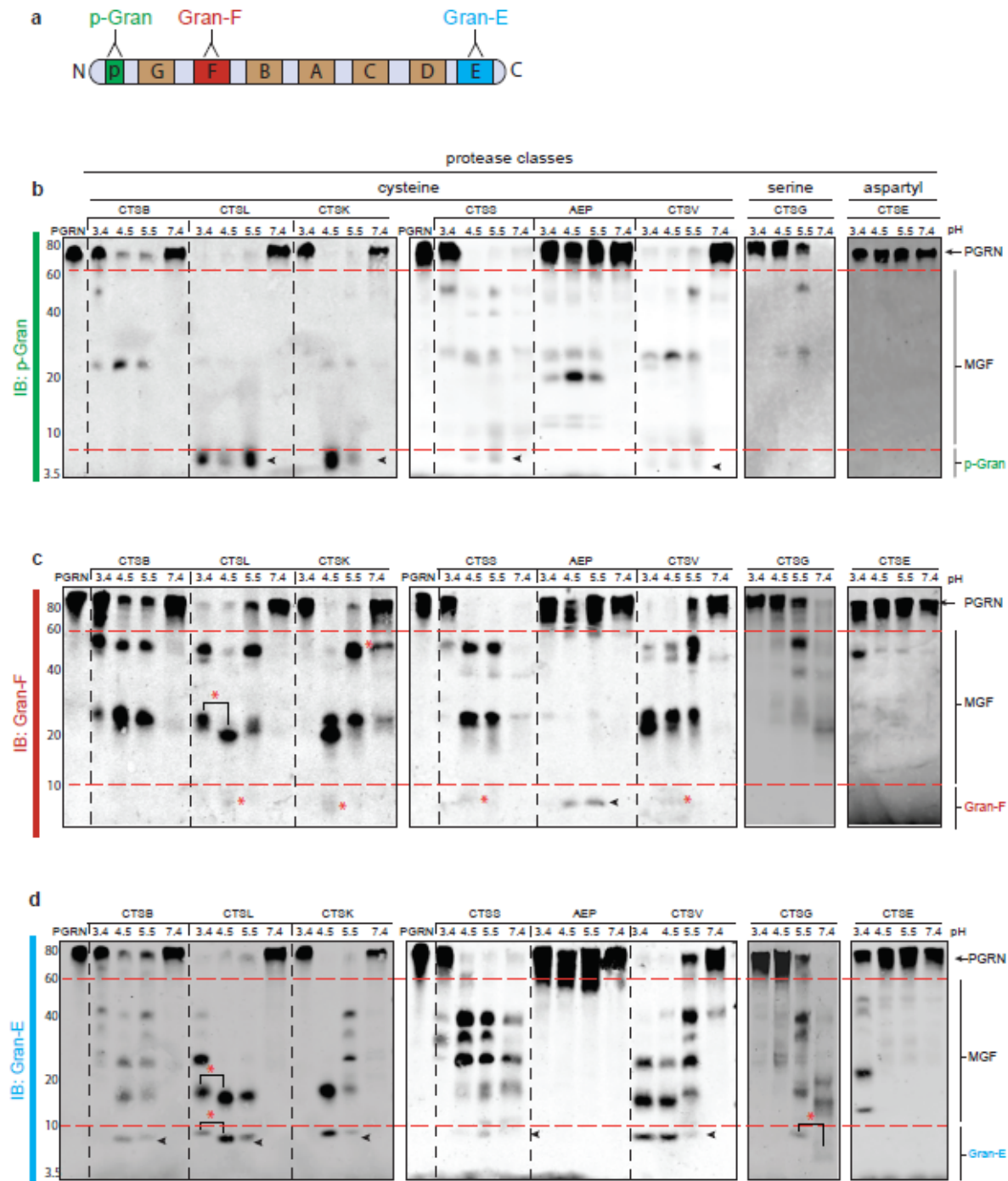
Figure 2

PGRN undergoes pH-dependent processing into multi-granulin fragments and individual granulins in vitro

a, Schematic representation of the antibodies used. Anti-paragranulin (p-Gran) in green, anti- granulin F (Gran-F) in red and anti-granulin E (Gran-E) in blue. b-d, For in vitro protease assays, 400ng of PGRN was

incubated for 20 minutes with or without 1μM of each enzyme at the indicated pH. Western blotting analysis was performed using antibodies as indicated. pH-dependent cleavage products are indicated with red asterisks (*). Progranulin (PGRN), multi-granulin fragments (MGFs), cathepsin B (CTSB), cathepsin L (CTSL), cathepsin K (CTSK), cathepsin S (CTSS), asparagine endopeptidase (AEP), cathepsin V (CTSV), cathepsin G (CTSG), cathepsin E (CTSE). A representative of N=3 replicates is shown.

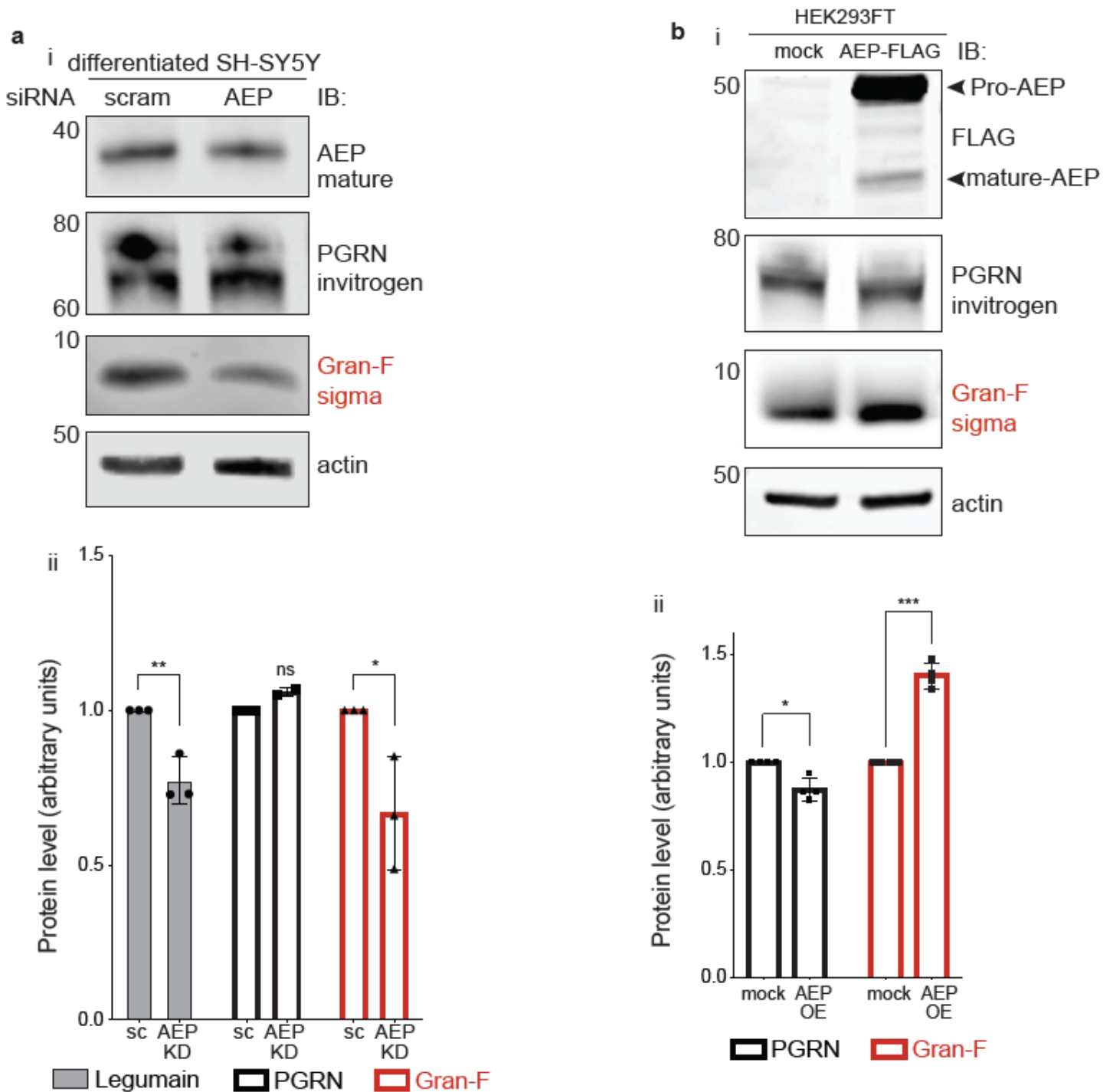## Figure 3. Asparagine endopeptidase is a PGRN protease that liberates granulins F

Figure 3

Asparagine endopeptidase is a PGRN protease that liberates granulin F a, Differentiated SH-SY5Y cells were treated with siRNA against AEP or scramble control for 60 hours. Cells were lysed and Western blotting performed for endogenous AEP, PGRN or Gran-F as indicated (i). Each biological replicate was run on a separate western blot and quantification (ii) was performed by normalizing each biological replicate against its corresponding mock control. Mature AEP and Gran-F levels were both significantly decreased (**p=0.006 and *p=0.03, respectively) relative to actin while endogenous PGRN levels were unaffected (ns, not-significant) Unpaired student's t-test, error bars represent mean with standard deviation, N=3. b, HEK293FT cells were transiently transfected with FLAG-tagged AEP or FLAG along for 24 hours and cells lysates were probed for endogenous PGRN and Gran-F (i). AEP expression was confirmed using an anti-FLAG antibody. Each biological replicate was run on a separate western blot and normalized to corresponding DMSO control. Endogenous PGRN and Gran-F levels were altered by AEP overexpression (**p=0.029 and ****p<0.0001, respectively). Unpaired student's t-test, error bars represent mean with standard deviation, N=4.

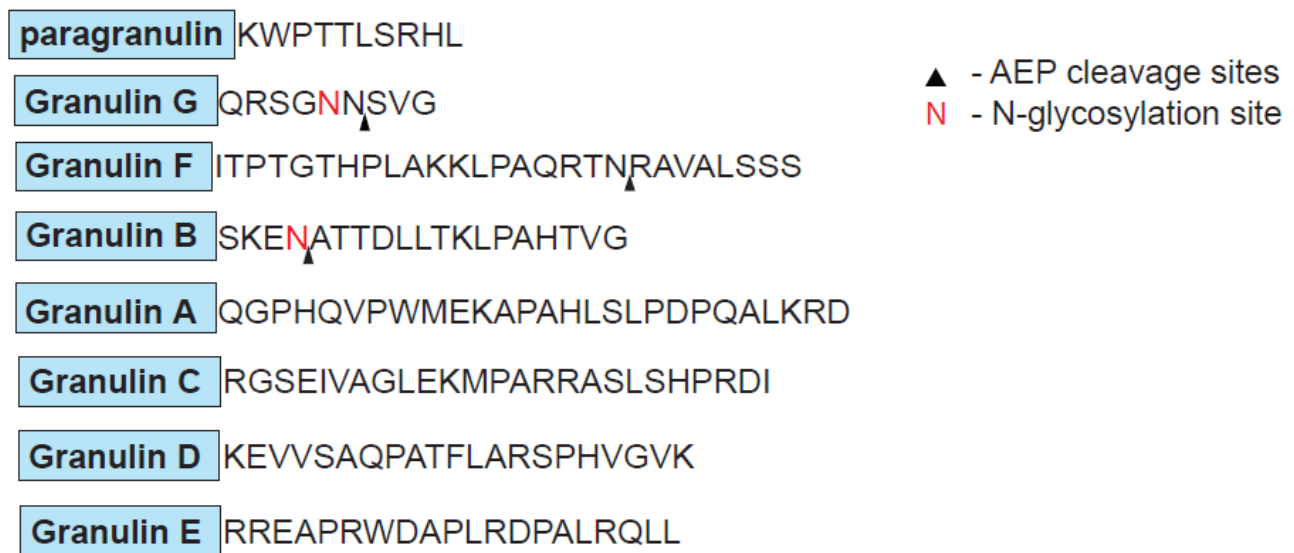## Figure 4. Asparagine endopeptidase liberates granulin F from progranulin

Figure 4

Asparagine endopeptidase liberates granulin F from PGRN Visual representation of PGRN protein with the individual granulin domains annotated in blue boxes with their associated C-terminal inter-granulin linker following. AEP cleavage sites are indicated with . N, represents N-linked glycosylation sites. PGRN, progranulin; Gran-F, granulin F.

Figure 5. Granulin F levels are significantly in degenerating brain of FTLD-TDP-*Pgrn* patients
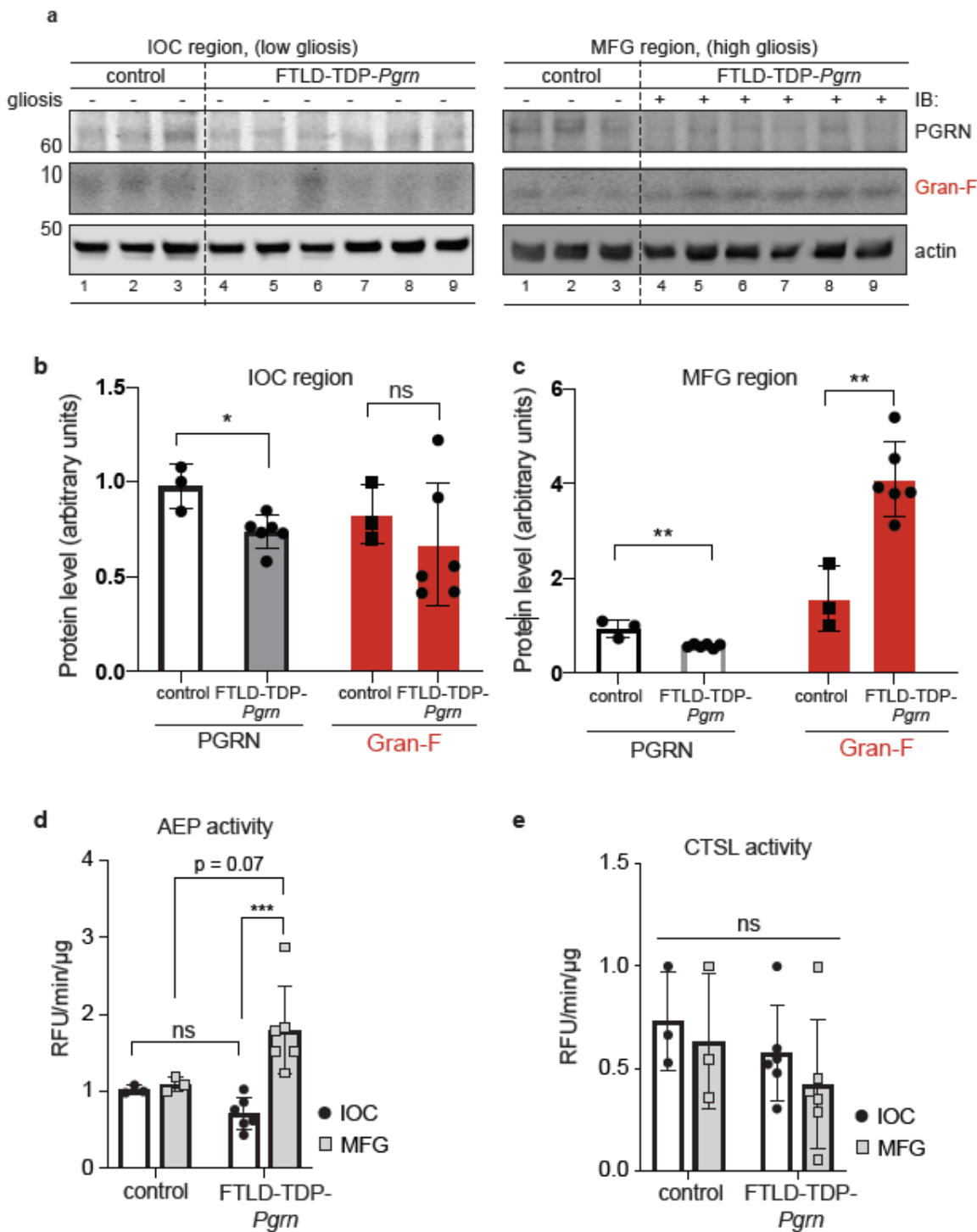
Figure 5

Granulins F levels are significantly increased in the degenerating regions of the brain from FTLD-TDP-Pgrn patients a, Western blot analysis of endogenous PGRN and Gran-F from human brain. b, Quantification of PGRN and Gran-F levels in IOC region in FTLD-TDP-Pgrn patients compared to the same regions in control subjects. (*, p=0.019). c, Quantification of PGRN and Gran-F levels in MFG regions in FTLD-TDP-Pgrn patients and controls (**, <p=0.0025). Error bars represent mean with standard deviation.

Multiple unpaired two-tailed student-t test was performed between each pair. d, AEP activity in both IOC and MFG regions in FTLD-TDP-Pgrn patients compared to the same regions in controls (***p=0.0008). One-way ANOVA was performed for statistical significance and Tukey's test was performed to correct for multiple comparisons. e, CTSL activity in both IOC and MFG regions in FTLD-TDP-Pgrn patients compared to the same regions in controls. ns, not significant. One-way ANOVA was performed for statistical significance and Tukey's test was performed to correct for multiple comparisons. PGRN, progranulin; Gran-F, granulin F. Sample numbers correspond to Table 2.

Supplementary Files

This is a list of supplementary files associated with this preprint. Click to download.

- AppendixFigureMohanetal.FINAL.pdf
- TABLESMohanetal.FINAL.pdf
- SupplementalFiguresMohanetal9Dec2020.pdf